

DiffVLA++: Bridging Cognitive Reasoning and End-to-End Driving through Metric-Guided Alignment

Yu Gao¹ Anqing Jiang^{1*} Yiru Wang¹ Heng Yuwen¹ Wang Shuo¹ Sun Hao¹ Wang Jijun²

¹RIX, Bosch ²AIR, Tsinghua University

Team: DiffVLA++

{Yu.Gao2, Anqing.JIANG, Yiru.WANG, Yuwen.HENG, Shuo.WANG8, Hao.SUN4}@cn.bosch.com

Abstract

Conventional end-to-end (E2E) driving models are effective at generating physically plausible trajectories, but often fail to generalize to long-tail scenarios due to the lack of essential world knowledge to understand and reason about surrounding environments. In contrast, Vision-Language-Action (VLA) models leverage world knowledge to handle challenging cases, but their limited 3D reasoning capability can lead to physically infeasible actions. In this work we introduce **DiffVLA++**, an enhanced autonomous driving framework that explicitly bridges cognitive reasoning and E2E planning through metric-guided alignment. First, we build a VLA module directly generating semantically grounded driving trajectories. Second, we design an E2E module with a dense trajectory vocabulary that ensures physical feasibility. Third, and most critically, we introduce a metric-guided trajectory scorer that guides and aligns the outputs of the VLA and E2E modules, thereby integrating their complementary strengths. The experiment on the ICCV 2025 Autonomous Grand Challenge leaderboard shows that DiffVLA++ achieves EPDMS of 49.12.

1. Introduction

End-to-end (E2E) autonomous driving frameworks have made significant progress in recent years by directly mapping multi-modal sensory inputs to control outputs or trajectories [1–13]. These models benefit from strong spatio-temporal modeling capabilities and are trained to produce physically plausible driving behaviors under normal operating conditions. However, they often struggle in long-tail scenarios due to their limited capacity for high-level scene understanding and semantic reasoning [14–17]. This weakness stems from their reliance on structured pattern recognition modules rather than human level cognitive modeling, leaving them devoid of generalizable world knowledge that

human drivers naturally exploit.

To address this limitation, recent work has explored Large Language Models (LLMs) and Vision-Language-Action (VLA) models in autonomous driving. Some studies using LLMs [18–20] rely on their extensive world knowledge to generate high-level planning decisions, while others [21–25] directly generate trajectories and thus constitute Vision-Language-Action (VLA) models. In DiffVLA++, we aim to leverage the VLA model to generate semantically rich, directly usable driving trajectories.

This raises a key challenge: while E2E models excel at physically grounded trajectory prediction and VLA models excel at cognitive reasoning with world knowledge, a principled way to bridge these two paradigms has not been fully explored. The difficulty lies in combining semantically rich but sometimes physically infeasible VLA trajectories with physically plausible but semantically limited E2E trajectories.

As shown in Fig. 1, we propose **DiffVLA++**, a framework that explicitly bridges reasoning and planning through a *metric-guided alignment mechanism*. We systematically compare VLA and E2E models on the NavsimV2 benchmark [26] and integrate their complementary strengths via the following components:

- **VLA Module:** A fully integrated and differentiable VLA model that generates semantically grounded trajectories with explicit 3D reasoning.
- **E2E Module:** A dense BEV-based E2E model with a transformer-based trajectory head, ensuring physical feasibility.
- **Metric-Guided Alignment:** An MLP-based trajectory scorer that shares the BEV feature space with the E2E module, regressing rule-based metrics such as No At-Fault Collisions (NC), Drivable Area Compliance (DAC), and aligning the trajectories from both VLA and E2E to unify their strengths.

Evaluations on the ICCV 2025 Autonomous Grand Challenge benchmark show that DiffVLA++ achieves Ex-

*Corresponding author: anqing.jiang@cn.bosch.com

tended Predictive Driver Model Score (EPDMS) [26] of 49.12.

2. Fully-Differentiable VLA Model for E2E Driving

The Vision-Language-Action (VLA) framework is designed around four core modules that jointly enable multimodal reasoning and trajectory generation.

The **visual processing stream** employs a CLIP-based Vision Transformer (ViT-L/14) that encodes multi-view images into a compact set of visual tokens. Each input image is resized and partitioned into patches, which are embedded into high-dimensional representations capturing spatial context. These tokens are then adapted through a Driving Vision Adapter that performs compression and projection, ensuring compatibility with the downstream language model.

In parallel, the **linguistic stream** encodes navigation commands and high-level driving instructions. A pretrained tokenizer first converts the input into subword units, which are then embedded and processed by a transformer-based text encoder. This produces text tokens that capture both semantic intent and syntactic dependencies.

The two modalities are integrated within a **large language model** (Vicuna-v1.5-7B), which performs multimodal fusion through a shared embedding space. Visual tokens are concatenated with text tokens, and the model employs causal attention to preserve autoregressive text generation while allowing cross-modal interactions. This design enables the model to jointly reason about visual observations and driving instructions in a unified space.

Finally, the last layer of the LLM projects the fused hidden states into continuous future trajectories of the ego vehicle. Instead of discretizing actions, the model directly predicts waypoints over a 4-second horizon, where each waypoint includes lateral position, longitudinal position, and heading angle. This fully differentiable design avoids discretization errors, improves smoothness, and allows end-to-end optimization of the driving policy.

To align with the E2E model (Sec. 3) and the metric-guided trajectory scorer (Sec. 4), features along the VLA-generated trajectory are sampled from the BEV feature map and fed into the trajectory scorer.

3. Conventional End-to-End Driving Model

The conventional end-to-end (E2E) driving module in our framework operates on a dense Bird’s Eye View (BEV) representation generated by BevFormer [27]. We adopt VoVNet-99 [28] as the image backbone to enhance the visual representational capacity. The BEV feature map is discretized into a 128×128 grid, covering a spatial extent of 64×64 meters along the ego-vehicle’s x and y axes.

Following the multi-task architecture of [2], the E2E module comprises three prediction heads: (i) an *agent detection head* that regresses the states of dynamic agents, (ii) a *semantic segmentation head* that predicts scene semantics in BEV space, and (iii) a *trajectory planning head* that generates the ego vehicle’s future motion.

The agent detection head employs a set of learnable agent queries $\mathbf{Q}_{\text{agent}} \in \mathbb{R}^{N \times d}$, which interact with the BEV features via deformable cross-attention to produce agent-centric embeddings $\mathbf{f}_a \in \mathbb{R}^{N \times d}$. These embeddings are decoded into bounding box parameters (x, y, w, l, θ) , representing the center coordinates, width, length, and heading of each detected agent. Together with the semantic segmentation output, this ensures that the BEV representation encodes both dynamic and contextual information for downstream planning (Sec. 3.1) and metric-guided alignment (Sec. 4).

3.1. Trajectory Planning Head

The trajectory planning head operates over a pre-defined dense trajectory vocabulary

$$\mathcal{V} \subset \mathbb{R}^{8192 \times 8 \times 3},$$

where each candidate trajectory $v \in \mathcal{V}$ consists of 8 waypoints sampled at 2 Hz over a four-second horizon. Each waypoint $\mathbf{p}_t = (x_t, y_t, \theta_t) \in \mathbb{R}^3$ encodes the 2D position and heading angle at time step t . The vocabulary \mathcal{V} is constructed via K -means clustering on expert trajectories from the navtrain split from Navsim dataset, ensuring broad coverage of feasible motion patterns.

For each candidate trajectory $v = \{\mathbf{p}_t\}_{t=0}^7$, BEV features are sampled at the waypoint locations using bilinear grid sampling. These features are aggregated into a compact trajectory-level embedding $\mathbf{f}_v \in \mathbb{R}^d$ via a learned fusion mechanism:

$$\begin{aligned} \mathbf{z}_v &= [\mathbf{F}(\mathbf{p}_0), \dots, \mathbf{F}(\mathbf{p}_7)] \in \mathbb{R}^{8 \times d}, \\ w &= \text{MLP}(\mathbf{s}_{\text{ego}}) \in \mathbb{R}^8, \\ \mathbf{f}_v &= \sum_{t=0}^7 w_t \mathbf{z}_v^{(t)}, \end{aligned}$$

where $\mathbf{F}(\mathbf{p}_t)$ denotes the BEV feature vector at position (x_t, y_t) , \mathbf{z}_v is the sequence of sampled waypoint features, \mathbf{s}_{ego} represents the current ego state (e.g., speed, acceleration, and high-level command concatenated and encoded using a MLP), and w_t is attention weight for t -th waypoint derived from \mathbf{s}_{ego} via an MLP. This design allows the fusion mechanism to emphasize waypoints that are more relevant to the current driving context.

To incorporate dynamic scene context, the trajectory embedding \mathbf{f}_v is further refined through cross-attention with

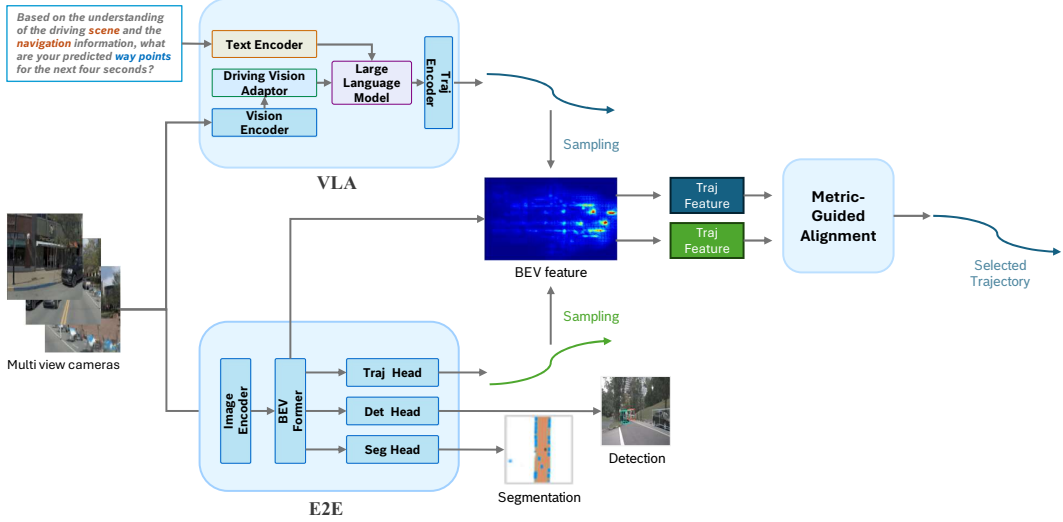


Figure 1. Overview of the DiffVLA++ architecture. It consists of three main components: (i) a VLA module, (ii) a conventional E2E module, both capable of directly generating planning trajectories, and (iii) a trajectory scorer that serves as a metric-guided aligner to unify their outputs.

both agent features \mathbf{f}_a and the ego state \mathbf{s}_{ego} :

$$\hat{\mathbf{f}}_v = \text{CrossAttn}(\text{CrossAttn}(\mathbf{f}_v, \mathbf{f}_a), \mathbf{s}_{\text{ego}}),$$

where $\hat{\mathbf{f}}_v$ denotes the context-enriched trajectory representation.

Finally, a decoding MLP transforms $\hat{\mathbf{f}}_v$ into a residual offset vector $\Delta v \in \mathbb{R}^{8 \times 3}$, comprising per-waypoint corrections $(\Delta x_t, \Delta y_t, \Delta \theta_t)$. The final output trajectory is obtained by:

$$v_{\text{pred}} = v + \Delta v.$$

In addition, the trajectory embedding \mathbf{f}_v is also used by the metric-guided trajectory scorer introduced in Sec. 4.

4. Metric-Guided Alignment

A key novelty of DiffVLA++ lies in **metric-guided alignment**, which serves as the bridge between the cognitively rich but sometimes physically infeasible trajectories from the VLA module and the physically grounded but semantically limited outputs of the E2E module. To achieve this, we employ a lightweight trajectory scorer that maps trajectory features into explicit driving metrics, thereby providing a shared evaluation space for both systems.

The trajectory scorer is implemented as a set of parallel MLP heads, each regressing one driving metric from the Navsim simulator. Given a trajectory feature \mathbf{f}_v , the scorer predicts \hat{s}_m for metric m :

$$\hat{s}_m = \text{MLP}_m(\mathbf{f}_v), \quad m \in \begin{cases} \text{NC, DAC, DDC, TLC,} \\ \text{EP, TTC, LK, HC.} \end{cases} \quad (1)$$

The simulator provides eight driving performance metrics, categorized as follows:

- EP (Ego Progress): continuous score in $[0, 1]$ measuring progress along the route centerline.
- DAC (Driveable Area Compliance), TLC (Traffic Light Compliance), TTC (Time-to-Collision), LK (Lane Keeping), HC (Hazard Compliance): binary scores in $\{0, 1\}$ indicating whether the ego vehicle violates specific driving rules.
- NC (Navigation Compliance), DDC (Dynamic Object Distance Compliance): ternary scores in $\{0, 0.5, 1\}$, where intermediate penalties are assigned when infractions are not directly caused by the ego vehicle.

The scorer is trained jointly with the E2E driving model, thereby correlating the BEV feature space with rule-based driving evaluations and providing auxiliary supervision for safer trajectory selection. Ground-truth metric labels are collected from the `navtrain` split of the Navsim dataset. Training minimizes a weighted regression objective:

$$\mathcal{L}_{\hat{s}} = \sum_{i,m} w_m \|\hat{s}_m^i - s_m^i\|_2^2,$$

where \hat{s}_m^i and s_m^i denote the predicted and ground-truth scores for metric m and the i -th trajectory, respectively, and w_m are per-metric weights balancing scale and importance.

By projecting both VLA-generated and E2E-generated trajectories into the same metric space, this scorer enables explicit alignment of VLA trajectories and E2E trajectories.

5. Post-Processing

We first employ a panoptic driving perception model [29] to predict the drivable area from the front-view camera. Can-

didate trajectories are projected into this view and discarded if they fall outside the predicted drivable area, serving as a safety check.

After this filtering step, the remaining candidate trajectories are each associated with predicted metric scores. We rank them by computing a weighted sum of the scores:

$$s_{\text{final}}^{\text{E2E}} = w_1 \cdot \hat{s}_{\text{NC}} + w_2 \cdot \hat{s}_{\text{DAC}} + w_3 \cdot \hat{s}_{\text{EP}} + w_4 \cdot \hat{s}_{\text{TTC}} + w_5 \cdot \hat{s}_{\text{LK}} + w_6 \cdot \hat{s}_{\text{DDC}}, \quad (2)$$

where the weights are empirically set to $w_1 = 4.0$, $w_2 = 0.8$, $w_3 = 0.01$, $w_4 = 0.1$, $w_5 = 0.04$, and $w_6 = 6.0$.

We then retain the top-ranked trajectory $traj_{\text{E2E}}$ from the E2E system as its final prediction. Similarly, the trajectory generated by the VLA module, $traj_{\text{VLA}}$, is evaluated using the same trajectory scorer to obtain $s_{\text{final}}^{\text{VLA}}$. Finally, the system selects the overall output trajectory by comparing $s_{\text{final}}^{\text{E2E}}$ and $s_{\text{final}}^{\text{VLA}}$, choosing either $traj_{\text{E2E}}$ or $traj_{\text{VLA}}$ as the final result. Due to time constraints of the competition, the two systems are combined through an offline ensemble.

6. Experiments

6.1. Training for VLA

For training the VLA model, we adopt the Vicuna-v1.5-7B backbone as the language model and a CLIP ViT-L/14 encoder as the visual backbone. Each input image is resized to 336×336 and divided into non-overlapping 14×14 patches, resulting in 196 patches per view. These patches are embedded into 1024-dimensional vectors, producing a sequence of 4096 visual tokens after multi-view concatenation. The Driving Vision Adapter further compresses projects into the joint embedding space of the LLM, producing a compact set of 1024 tokens.

The linguistic input is first tokenized using the LLama tokenizer with a vocabulary size of 32,000. The resulting text tokens are embedded into 1024 text tokens before being fused with visual tokens in the multimodal transformer. The language model has 32 transformer layers, 32 attention heads, and a hidden size of 4096, leading to approximately 7B trainable parameters.

We train the VLA module end-to-end and the model directly regresses future waypoints over a 4-second horizon at 2 Hz, where each waypoint includes (x, y, θ) . Training is performed using AdamW [30] with a cosine learning rate schedule [31], an initial learning rate of 1×10^{-5} . A dropout rate of 0.05 is applied to both the vision adapter and the LLM. The VLA model is trained for 1 epoch with a batch size of 8 across 8 NVIDIA A800 GPUs.

6.2. Training for E2E and scorer in Metric-Guided Alignment

The E2E module and the trajectory scorer are trained jointly to ensure a consistent BEV feature space that captures both

semantic and dynamic scene information. The overall training objective includes the following components: agent bounding box regression loss, agent classification loss, semantic segmentation loss, trajectory imitation loss, and scorer loss. We assign loss weights as follows: 1.0 for agent bounding box regression, 10.0 for agent classification, 20.0 for trajectory imitation, 14.0 for semantic segmentation, and 14.0 for the scorer. The model is trained for 30 epochs with a total batch size of 8 and an initial learning rate of 1×10^{-4} on 8 A800 GPUs. The E2E module use same optimizer and learning rate schdular as VLA module.

6.3. Experiments result

We present the performance of the VLA and E2E modules on the Navhard two-stage test in Tab. 1 and results of final ensembled model in the public leaderboard in Tab. 2

Table 1. Results of different Branches in DiffVLA++ on Navhard Two Stage Test.

Models	EPDMS
VLA Branch	48.0
E2E Branch	43.7

Table 2. Results of DiffVLA++ on the Public Leaderboard

Metric Name	Scores
extended_pdm_score_combined	49.1238
no_at_fault_collisions_stage_one	98.2143
drivable_area_compliance_stage_one	98.5714
driving_direction_compliance_stage_one	100
traffic_light_compliance_stage_one	99.2857
ego_progress_stage_one	79.5117
time_to_collision_within_bound_stage_one	98.5714
lane_keeping_stage_one	95
history_comfort_stage_one	92.8571
two_frame_extended_comfort_stage_one	50
no_at_fault_collisions_stage_two	88.7709
drivable_area_compliance_stage_two	95.3235
driving_direction_compliance_stage_two	97.2196
traffic_light_compliance_stage_two	98.1711
ego_progress_stage_two	73.4289
time_to_collision_within_bound_stage_two	87.9888
lane_keeping_stage_two	59.4454
history_comfort_stage_two	98.9833
two_frame_extended_comfort_stage_two	52.9822

7. Conclusion

In this work, We propose **DiffVLA++**, a framework that combines the strengths of VLA and E2E autonomous driving models through metric-guided alignment. By aligning the two systems, our approach achieves an EPDMS of 49.12, surpassing both standalone E2E and VLA models.

References

[1] S. Hu, L. Chen, P. Wu, H. Li, J. Yan, and D. Tao, “St-p3: End-to-end vision-based autonomous driving via spatial-temporal feature learning,” in *European Conference on Computer Vision*. Springer, 2022, pp. 533–549. [1](#)

[2] K. Chitta, A. Prakash, B. Jaeger, Z. Yu, K. Renz, and A. Geiger, “Transfuser: Imitation with transformer-based sensor fusion for autonomous driving,” *IEEE transactions on pattern analysis and machine intelligence*, vol. 45, no. 11, pp. 12 878–12 895, 2022. [2](#)

[3] B. Jiang, S. Chen, Q. Xu, B. Liao, J. Chen, H. Zhou, Q. Zhang, W. Liu, C. Huang, and X. Wang, “Vad: Vectorized scene representation for efficient autonomous driving,” in *Proceedings of the IEEE/CVF International Conference on Computer Vision*, 2023, pp. 8340–8350.

[4] W. Tong, C. Sima, T. Wang, L. Chen, S. Wu, H. Deng, Y. Gu, L. Lu, P. Luo, D. Lin *et al.*, “Scene as occupancy,” in *Proceedings of the IEEE/CVF International Conference on Computer Vision*, 2023, pp. 8406–8415.

[5] Y. Hu, J. Yang, L. Chen, K. Li, C. Sima, X. Zhu, S. Chai, S. Du, T. Lin, W. Wang *et al.*, “Planning-oriented autonomous driving,” in *Proceedings of the IEEE/CVF conference on computer vision and pattern recognition*, 2023, pp. 17 853–17 862.

[6] W. Sun, X. Lin, Y. Shi, C. Zhang, H. Wu, and S. Zheng, “Sparsedrive: End-to-end autonomous driving via sparse scene representation,” *arXiv preprint arXiv:2405.19620*, 2024.

[7] X. Weng, B. Ivanovic, Y. Wang, Y. Wang, and M. Pavone, “Para-drive: Parallelized architecture for real-time autonomous driving,” in *Proceedings of the IEEE/CVF Conference on Computer Vision and Pattern Recognition*, 2024, pp. 15 449–15 458.

[8] Z. Li, K. Li, S. Wang, S. Lan, Z. Yu, Y. Ji, Z. Li, Z. Zhu, J. Kautz, Z. Wu *et al.*, “Hydra-mdp: End-to-end multimodal planning with multi-target hydra-distillation,” *arXiv preprint arXiv:2406.06978*, 2024.

[9] Y. Li, L. Fan, J. He, Y. Wang, Y. Chen, Z. Zhang, and T. Tan, “Enhancing end-to-end autonomous driving with latent world model,” *ICLR*, 2025.

[10] B. Liao, S. Chen, H. Yin, B. Jiang, C. Wang, S. Yan, X. Zhang, X. Li, Y. Zhang, Q. Zhang *et al.*, “Diffusiondrive: Truncated diffusion model for end-to-end autonomous driving,” in *Proceedings of the Computer Vision and Pattern Recognition Conference*, 2025, pp. 12 037–12 047.

[11] Z. Xing, X. Zhang, Y. Hu, B. Jiang, T. He, Q. Zhang, X. Long, and W. Yin, “Goalflow: Goal-driven flow matching for multimodal trajectories generation in end-to-end autonomous driving,” in *Proceedings of the Computer Vision and Pattern Recognition Conference*, 2025, pp. 1602–1611.

[12] K. Li, Z. Li, S. Lan, Y. Xie, Z. Zhang, J. Liu, Z. Wu, Z. Yu, and J. M. Alvarez, “Hydra-mdp++: Advancing end-to-end driving via expert-guided hydra-distillation,” *arXiv preprint arXiv:2503.12820*, 2025.

[13] W. Zheng, R. Song, X. Guo, C. Zhang, and L. Chen, “Genad: Generative end-to-end autonomous driving,” in *European Conference on Computer Vision*. Springer, 2024, pp. 87–104. [1](#)

[14] D. Fu, X. Li, L. Wen, M. Dou, P. Cai, B. Shi, and Y. Qiao, “Drive like a human: Rethinking autonomous driving with large language models,” in *2024 IEEE/CVF Winter Conference on Applications of Computer Vision Workshops (WACVW)*. IEEE, 2024, pp. 910–919. [1](#)

[15] X. Zhou, M. Liu, E. Yurtsever, B. L. Zagar, W. Zimmer, H. Cao, and A. C. Knoll, “Vision language models in autonomous driving: A survey and outlook,” *IEEE Transactions on Intelligent Vehicles*, 2024.

[16] T. Cai, Y. Liu, Z. Zhou, H. Ma, S. Z. Zhao, Z. Wu, and J. Ma, “Driving with regulation: Interpretable decision-making for autonomous vehicles with retrieval-augmented reasoning via llm,” *arXiv preprint arXiv:2410.04759*, 2024.

[17] L. Chen, P. Wu, K. Chitta, B. Jaeger, A. Geiger, and H. Li, “End-to-end autonomous driving: Challenges and frontiers,” *IEEE Transactions on Pattern Analysis and Machine Intelligence*, 2024. [1](#)

[18] W. Wang, J. Xie, C. Hu, H. Zou, J. Fan, W. Tong, Y. Wen, S. Wu, H. Deng, Z. Li *et al.*, “Drivelm: Aligning multi-modal large language models with behavioral planning states for autonomous driving,” *arXiv preprint arXiv:2312.09245*, 2023. [1](#)

[19] X. Tian, J. Gu, B. Li, Y. Liu, Y. Wang, Z. Zhao, K. Zhan, P. Jia, X. Lang, and H. Zhao, “Drivevlm: The convergence of autonomous driving and large vision-language models,” *arXiv preprint arXiv:2402.12289*, 2024.

[20] B. Jiang, S. Chen, B. Liao, X. Zhang, W. Yin, Q. Zhang, C. Huang, W. Liu, and X. Wang, “Senna: Bridging large vision-language models and end-to-end autonomous driving,” *arXiv preprint arXiv:2410.22313*, 2024. [1](#)

[21] J.-J. Hwang, R. Xu, H. Lin, W.-C. Hung, J. Ji, K. Choi, D. Huang, T. He, P. Covington, B. Sapp *et al.*, “Emma: End-to-end multimodal model for autonomous driving,” *arXiv preprint arXiv:2410.23262*, 2024. [1](#)

[22] H. Fu, D. Zhang, Z. Zhao, J. Cui, D. Liang, C. Zhang, D. Zhang, H. Xie, B. Wang, and X. Bai, “Orion: A holistic end-to-end autonomous driving framework by

vision-language instructed action generation,” *arXiv preprint arXiv:2503.19755*, 2025.

- [23] Y. Li, K. Xiong, X. Guo, F. Li, S. Yan, G. Xu, L. Zhou, L. Chen, H. Sun, B. Wang *et al.*, “Recogdrive: A reinforced cognitive framework for end-to-end autonomous driving,” *arXiv preprint arXiv:2506.08052*, 2025.
- [24] Z. Zhou, T. Cai, S. Z. Zhao, Y. Zhang, Z. Huang, B. Zhou, and J. Ma, “Autovla: A vision-language-action model for end-to-end autonomous driving with adaptive reasoning and reinforcement fine-tuning,” *arXiv preprint arXiv:2506.13757*, 2025.
- [25] S. Jiao, K. Qian, H. Ye, Y. Zhong, Z. Luo, S. Jiang, Z. Huang, Y. Fang, J. Miao, Z. Fu *et al.*, “Evadive: Evolutionary adversarial policy optimization for end-to-end autonomous driving,” *arXiv preprint arXiv:2508.09158*, 2025. 1
- [26] W. Cao, M. Hallgarten, T. Li, D. Dauner, X. Gu, C. Wang, Y. Miron, M. Aiello, H. Li, I. Gilitschenski *et al.*, “Pseudo-simulation for autonomous driving,” *arXiv preprint arXiv:2506.04218*, 2025. 1, 2
- [27] Z. Li, W. Wang, H. Li, E. Xie, C. Sima, T. Lu, Q. Yu, and J. Dai, “Bevformer: learning bird’s-eye-view representation from lidar-camera via spatiotemporal transformers,” *IEEE Transactions on Pattern Analysis and Machine Intelligence*, 2024. 2
- [28] Y. Lee and J. Park, “Centermask: Real-time anchor-free instance segmentation,” in *Proceedings of the IEEE/CVF conference on computer vision and pattern recognition*, 2020, pp. 13 906–13 915. 2
- [29] J. Wang, Q. Wu, K. Suto, and N. Zhang, “Rmt-ppad: Real-time multi-task learning for panoptic perception in autonomous driving,” *arXiv preprint arXiv:2508.06529*, 2025. 3
- [30] I. Loshchilov and F. Hutter, “Decoupled weight decay regularization,” *arXiv preprint arXiv:1711.05101*, 2017. 4
- [31] ———, “Sgdr: Stochastic gradient descent with warm restarts,” *arXiv preprint arXiv:1608.03983*, 2016. 4